DELIVERABLE 5.16

CONTRACT N°	**TIP4-CT-2005-516420**
PROJECT N°	**FP6-516420**
ACRONYM	**QCITY**
TITLE	**Quiet City Transport**
Subproject 5	**Design and Implementation of Solution at Validation Sites**
Work Package 5.11	**Test of new quiet passenger tyre designs**
	Deliverable 5.16 An analytical model for calculating the vibration response and sound radiation from an in-service tyre/road system: The analytical model and calculated results
Written by	**Professor Ann Dowling, University of Cambridge UCAM**
Date of issue of this report	**16th December 2008**

PROJECT CO-ORDINATOR PARTNERS			
	Acoustic Control	ACL	SE
	Accon	ACC	DE
	Akron	AKR	BE
	Amec Spie Rail	AMEC	FR
	Alfa Products & Technologies	APT	BE
	Banverket	BAN	SE
	Composite Damping Material	CDM	BE
	Havenbedrijf Oostende	HOOS	BE
	Frateur de Pourcq	FDP	BE
	Goodyear	GOOD	LU
	Head Acoustics	HAC	DE
	Heijmans Infra	HEIJ	BE
	Royal Institute of Technology	KTH	SE
	Vlaamse Vervoersmaatschappij DE LIJN	LIJN	BE
	Lucchini Sidermeccanica	LUC	IT
	NCC Roads	NCC	SE
	Stockholm Environmental & Health Administration	SEA	SE
	Société des Transports Intercommunaux de Bruxelles	STIB	BE
	Netherlands Organisation for Applied Scientific Research	TNO	NL
	Trafikkontoret Göteborg	TRAF	SE
	Tram SA	TRAM	GR
	TT&E Consultants	TTE	GR
	University of Cambridge	UCAM	UK
	University of Thessaly	UTH	GR
	Voestalpine Schienen	VAS	AU
	Zbloc Norden	ZBN	SE
	Union of European Railway Industries	UNIFE	BE

PROJECT START DATE **February 1, 2005**

DURATION **48 months**

Project funded by the European Community under the SIXTH FRAMEWORK PROGRAMME
PRIORITY 6
Sustainable development, global change & ecosystems

This deliverable has been quality checked and approved by QCITY Coordinator
Nils-Åke Nilsson

TABLE OF CONTENTS

0 EXECUTIVE SUMMARY

The modelling approach developed by UCAM for the prediction of tyre vibration and radiated noise is summarised. Results are given for a generic tyre and various low noise concepts are investigated. The effects of changes in tyre radius and width are presented. A decrease in tyre width is particularly beneficial to reduce radiated sound because it leads to reductions in both the mechanical vibration and the horn effect. The twin-tyre concept provides a practical way of implementing that while keeping the same load on the tyre. Such a change is predicted to lead of about 6.5-8.5 dBA reduction (3.5 dBA from the reduction in the mechanical vibration and 3-5 dBA in total from the horn effect, with 1-2 dBA of this being from changes in the shoulder curvature). A polyurethane-filled tyre is also considered and found to be beneficial for noise but to be impractical due to its additional weight.

0.1 OBJECTIVE OF THE DELIVERABLE

This Deliverable summaries the modelling approach developed by UCAM for tyre noise and vibration and gives results for a generic tyre, illustrating the effects of some of the changes that might be made for noise reduction; geometrical change; in-fill with a polyurethane material and a twin-tyre concept.

1 INTRODUCTION

The noise radiated from pneumatic car tyres is one of the most significant local environmental issues in Europe [1]. The amplitude and frequency content of this noise is a function of many parameters, including the road surface texture, tyre dimensions, tyre materials and construction and the tread pattern.

In the EU Quiet City Transport research project, the modelling capability at UCAM has been used to investigate the noise from variety of different tyres. In particular, possible noise reduction mechanisms have been investigated including the impact of tyre diameter and width; a polyurethane rubber in-fill and a twin-tyre concept.

2 MODELLING APPROACH

In order to be able to predict the sound radiated from the tyre, it is necessary to be able to obtain the response of the tyre to arbitrary forcing and then to describe the sound radiated by the tyre belt vibration as the tyre rolls over a rough surface. The radiation problem includes determining the horn amplification by the geometry of the tyre-road contact geometry. The modelling approach is decomposed into the inter-related elements discussed below.

2.1 BELT VIBRATION

A numerical method has been developed [2, 3] which provides the modal response of both the tyrebelt and the response of the finite width tyre, taking into account the impact of the sidewalls, to an arbitrary force applied to the outer surface of the tyre belt.

2.1.1 Viscoelastic cylindrical model

The modal response of a tyre belt can be determined using a viscoelastic cylindrical model [2, 3] which takes into account the properties of each layer of tyre materials. A typical tyre belt is illustrated in Fig. 1. It is made of several layers of material laid on top of each other, including steel cords and rubber layers. In this figure, there is an air cavity joining the tyre belt to a fixed axle hub but the model can equally well be used for a tyre with a polyurethane rubber in-fill. A load σ_{rr} is applied to the outer surface of the tyre belt in a radial direction and the displacement response u_r is to be determined as a function of the excitation frequency ω, axial wavenumber k_z and angular order n (these are the modes of vibration in the spanwise, ie across the tyre width, and circumferential directions respectively).

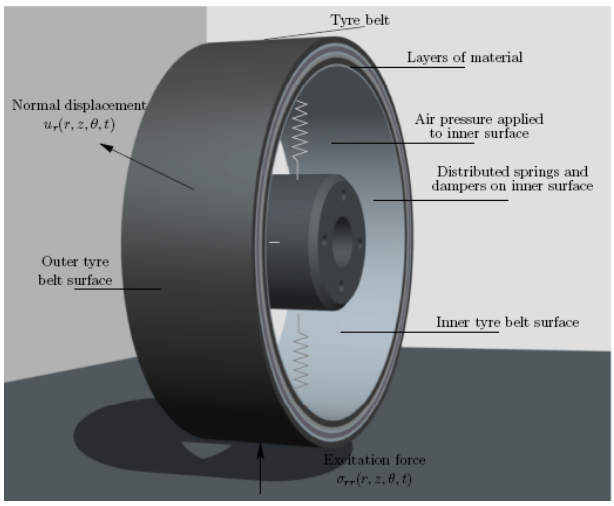

Fig. 1 Viscoeleastic cylindrical model of tyrebelt for modal analysis

Each layer of the material is represented using the viscoelastic stress-strain relations, with the components of displacement $\mathbf{u}$ and traction $\boldsymbol{\sigma}$ on the outer surface of the layer related to those on the inner surface through a propagation matrix $\mathbf{X}$. This propagation matrix contains information on the stiffness of the layer j, the excitation frequency and the dimensions of the layer (the outer radius is denoted r_{j+1} and the inner radius r_j).

$$\begin{pmatrix} \tilde{\sigma} \\ \tilde{\mathrm{u}} \end{pmatrix}_{r_{j+1}} = \mathbf{X}_j \begin{pmatrix} \tilde{\sigma} \\ \tilde{\mathrm{u}} \end{pmatrix}_{r_j}. \qquad (1)$$

The tyre belt structure is made up of several layers of different material laid on top of each other. We assume a common displacement and stress at the interface between layers. This allows an overall representation of the tyre belt to be written between the stress and displacement components on the most outer layer (in contact with the road and atmosphere) to those on the most inner surface (in contact with an air cavity, say),

$$\begin{pmatrix} \tilde{\sigma} \\ \tilde{\mathrm{u}} \end{pmatrix}_{r_{N+1}} = \prod_{j=1}^{N} \mathbf{X}_j \begin{pmatrix} \tilde{\sigma} \\ \tilde{\mathrm{u}} \end{pmatrix}_{r_1}. \qquad (2)$$

The overall matrix contains Bessel's functions which represent the different wave speeds in the layers, so that the model can represent both the dominant flexural and compression waves found in the tyre belt structure. It is therefore valid for any thickness of layer and can provide results over a wide frequency range (we limit the analysis to frequencies below 2.5 kHz).

In order to determine the displacement response to force excitation, we must assign boundary conditions to the tyre belt. On the inner surface, we assume that the air cavity and sidewalls provide a force proportional to the displacement of the inner surface which is distributed over the width of the tyre belt. This Winkler foundation is a simplification; however for the purposes of studying the effect of a radial change with no change in the axial dimension, it is valid.

On the outer surface we assume that the air in contact with the tyre belt cannot provide any shear forces to the tyre. We apply a radial force to the outer surface of the tyre belt σ_{rr} to obtain the displacement in the frequency domain $u_r(\omega)$. Inverse Fourier transform routines are used to invert the response from functions of angular order n back to circumferential position θ.

2.1.2 Description of the finite width tyre model

To obtain the frequency response of the tyre with sidewalls, a finite width bending plate model is utilised from Blakemore (for a detailed description see [2-6]), which provides the response of the tyre in the radial direction when excited in the radial direction at a range of axial positions across the tread width. It yields the Green's function G_{mn} required to determine the response of the tyre as it rolls at speed (the Green's function provides the response at tread block m to an impact at tread block n).

The model of the finite width tyre is provided by using a flat bending orthotropic plate. The bending plate has parameters including bending stiffness, in-plane tension and

damping which may be adjusted to yield the equivalent response as a tyre when forced in a direction normal to the surface. The equations for the bending plate only allow the dominant flexural wave to be studied, neglecting the impact of shear excitation and compression waves; however, for normal forcing and normal displacement response, this is a valid assumption.

With reference to Fig. 2, the equation of motion for the bending plate in formulated in terms of a displacement w relating to an excitation force/unit plate area p and is given by,

$$B_{xxxx}\frac{\partial^4 w}{\partial x^4}+(B_{xxyy}+B_{xyxy})\frac{\partial^4 w}{\partial x^2\partial y^2}+B_{yyyy}\frac{\partial^4 w}{\partial y^4}-T_x\frac{\partial^2 w}{\partial x^2}-T_y\frac{\partial^2 w}{\partial y^2}$$

$$-\eta\frac{\partial}{\partial t}(C_{xx}\frac{\partial^2 w}{\partial x^2}+C_{yy}\frac{\partial^2 w}{\partial y^2})+M\frac{\partial^2 w}{\partial t^2}+\frac{k_i}{2\pi RW}\int\int w dxdy=p(x,y,t), \quad (3)$$

where k_i is the tyre inflation pressure integrated over the width of the tyre W, with in-plane tensions T_x, T_y, damping loss factor η, constants C_{xx}, C_{yy}, bending stiffness B and mass of the tyre M.

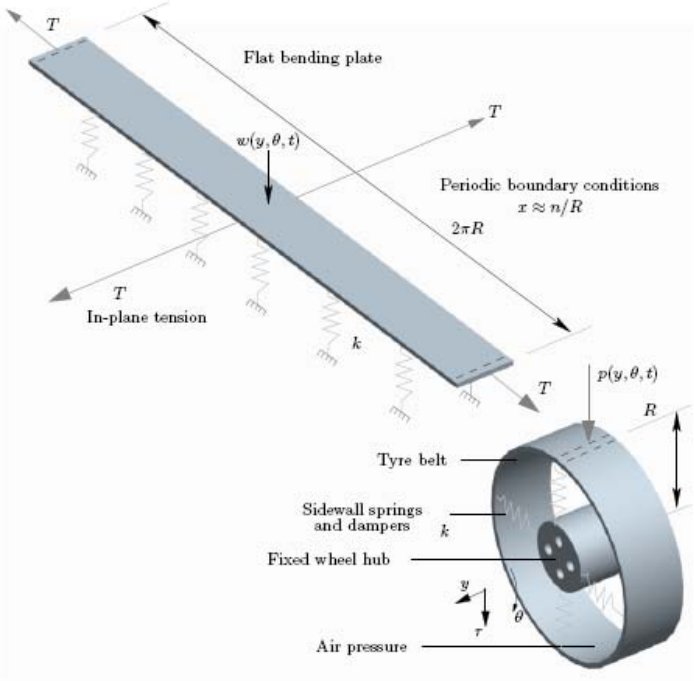

Fig. 2 The bending plate model of tyre response

The model requires that Fourier transforms are taken in time t and circumferential position x to frequency ω and n respectively. Blakemore then applies boundary conditions to the plate to create a representative model of a finite width tyre with sidewalls. At the sides of the tyre, there are no moments, only normal forces proportional to the stiffness of sidewall springs k. The number of boundary conditions applied to the edges of the plate provides a limit on the number of wavelengths in the span-wise direction.

Once the material parameters are applied to the equations, the boundary conditions may be applied to solve for w in the Fourier domain. A simple inverse Fourier transform then yields the displacement of the finite width tyre in the time domain.

2.1.3 Rolling tyre vibration

The finite bending plate model has provided numerical data on the displacement response of a tread block m on the tyre to forcing at a tread block n. This transfer function G_{mn} is calculated for every tread block combination on the tyre, as a regular distribution of 280 blocks arranged in five rows across the tyre width.

The prediction of the vibration of a tyre rolling on a rough road surface has been carried out by O'Boy [2, 3] and Graf [4, 5], using a convolution method in the time domain of the tyre response and the force from the road through the tread blocks. The displacement of the tread blocks and the surface of the tyre belt as a function of time, as they move over a rough road surface, are obtained using the time stepping method developed by Dowling et al [6] and Kropp [7, 8]. The geometry and notation are shown in Fig. 3 and $u_m^{belt}(t)$, the displacement of the tyre belt at a block m at time t due to an applied force $f_n(\tau)$ at block n at time τ, is determined by the convolution summed over N tread blocks,

$$u_m^{belt}(t) = \sum_{n=1}^{N} \int_{-\infty}^{t} G_{mn}(t-\tau)\ f_n(\tau)\, d\tau$$

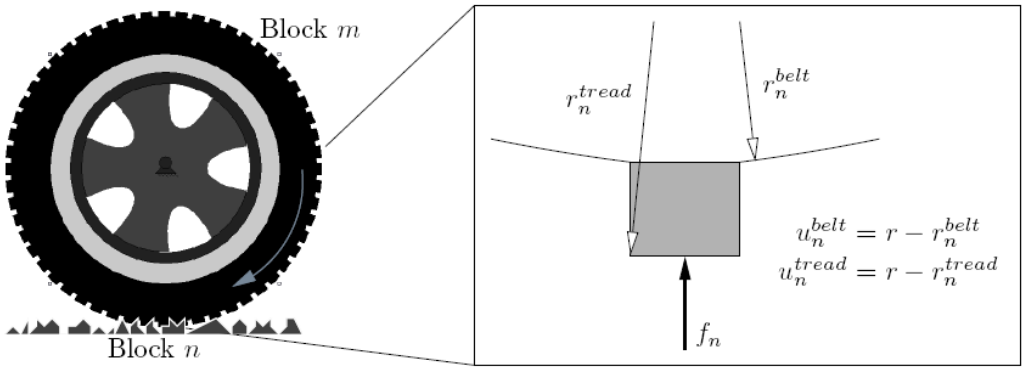

Fig. 3. Notation used to define the displacements of the tyre belt and tread blocks as they roll over a rough road surface.

The forcing function, $f_n(\tau)$, is calculated based on the displacement of the tyre belt u_n^{belt}, the tread block height H_{blk} and the road surface height u_n^{tread}. When the tread block of stiffness k_{blk} is out of contact with the road, this force is set to zero otherwise it may be calculated using

$$f_n = k_{blk}(H_{blk} + u_n^{tread} - u_n^{belt}) .$$

The time stepping routine requires a known set of initial conditions at time $t = 0$. The tyres are initialised out of contact with the ground as they rotate, where the force from the road surface is known to be zero. The time stepping routine then slowly lowers the tyre by a set amount, until the overall load on the axle matches the required tyre load (420 kg determined empirically). Several further rotations of the tyre are allowed before results are output, in order to allow any transient vibrations to decay. It is assumed that all tread block rows are designed to carry the same load for steady state rolling conditions with no steering input. For each numerical analysis on different road surfaces, 1500 computation time steps are utilised per revolution of the tyre in order to resolve the important vibration data between the road and the tyre belt.

2.2 SOUND PREDICTION

This section describes the method used to obtain predictions of the radiated sound from the tyre, using the tyre vibration determined as described in Section 2.1.3.

Once the radial acceleration $a(\underline{x},\omega)$ at a position $\underline{x}$ on the tyre surface is known, the far-field sound pressure may be predicted by first assuming that we have a distribution of sources above a rigid plane without any solid tyre geometry. This may then be combined with G_{horn} a transfer function describing the amplification from the horn shape created between the tyre and road surface. If the receiver position is located at $\underline{y}$ with an element of tyre surface at $\underline{x}$ of area ΔA, then we may write for the sound pressure $p'(\underline{y},\omega)$;

$$p'(\underline{y},\omega) = \frac{\rho_0}{2\pi}\sum a(\underline{x},\omega)\frac{e^{-ik|\underline{y}-\underline{x}|}}{|\underline{y}-\underline{x}|}G_{horn}(\underline{x},\omega)\Delta A \qquad (4)$$

To calculate the horn amplification a commercial boundary element code (BEM) is used (*Comet Acoustics v5.1*). Such results for the horn amplification have been previously validated by comparison against experimental measurements with good agreement for a wide range of frequencies covering the range of interest for exterior tyre / road noise [9].

The details of the BEM are provided by [10] and [11] for both the direct and indirect methods, the latter are preferable for exterior calculations since they give a computational speed advantage. The tyre geometry meshes were unstructured with approximately 6000 nodes and special O-grid rings on the sidewalls to improve the convergence speed and reliability of the results (the O-grid reduces the cell density as the meshing radius tends to zero). The geometry was designed using *ProE* and the surface meshing carried out using *ICEM-CFD*.

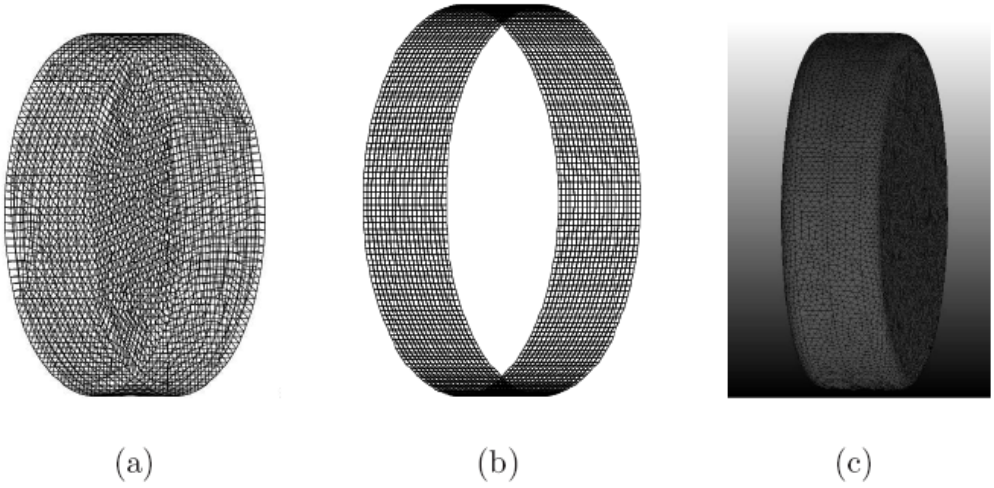

Fig 4. Illustrations of the meshes used in the boundary element calculations; (a) Geometry mesh (b) Data recovery mesh (c) High density geometry mesh used to check mesh independence.

The density of the mesh must be high enough to resolve the maximum frequency of interest with at least four elements per wavelength. The maximum acoustic frequency of interest for tyre noise is 2.5 kHz, which determined the mesh used for all standard results (Fig. 4(a)). However, to verify that the solution was mesh independent comparison was made with the solution on a mesh with four times as many surface nodes (Fig. 4(c)). The results were virtually identical except inside the contact patch where the solution failed to converge for either case (it is assumed that there is no vibration inside the contact patch which radiates sound so this does not influence the results).

In both the experimental and numerical cases, it is useful to employ the reciprocal method to exchange the position of the source and receiver [12]. The designated microphone positions given in the results are therefore the locations of a single monopole source, with unit magnitude and the receiver positions are represented by a data recovery mesh consisting of approximately 4000 nodes positioned at a distance of at least one quarter of an element length away from the tyre geometry mesh. This is a structured mesh generated in *Matlab* (see Fig. 4b)) and allows simple data recovery and processing outside the *Comet* code.

The advantage of the boundary element calculation is that only the boundary conditions on the surface of the geometry need to be defined. In all of the calculations carried out, each element of the tyre geometry was defined to have zero normal velocity, as a rigid surface. A half plane was placed at the base of the tyre with an impedance of 1×10^{10} kg/m^{2}s which could be adjusted vertically to reduce or increase the length of the contact patch. The half plane represents a rigid smooth surface with no porosity.

3 RESULTS

3.1 VIBRATION RESPONSE

3.1.1 Modal response of the tyre with a change in the tyre radius

The radial response of a tyre is shown in Fig. 5 for the case where the excitation is applied radially in the centre of the trye width and the response is calculated at the same position. The results for three tyres of different radii are shown. The larger the radius the greater the reduction in the amplitude of the resonances at higher frequencies, with reductions seen even at the third axial (ie spanwise) mode shape of around 650 Hz. The amplitudes at lower frequencies remain largely similar although the sharpness of the peaks increases below 500 Hz. At higher frequencies it can also be seen that the damping in the tyre belt means that the response is insignificant away from the forcing location (see Fig. 6).

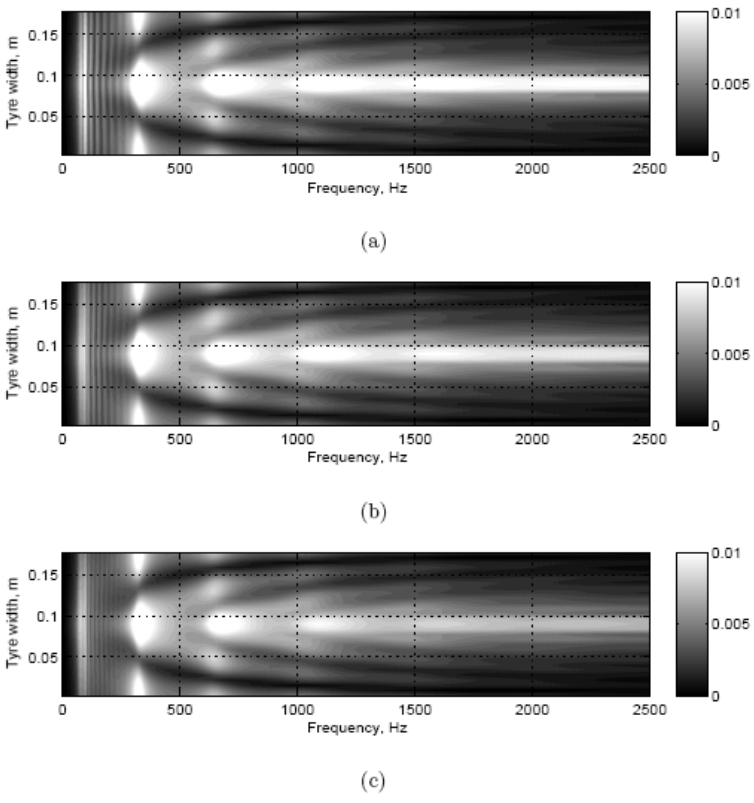

Fig. 5. Tyre normal velocity for excitation radially at the centre of the tread and measuring across tread points v_r / σ_{rr} 10^9 m^3/Ns*. Both forcing and measurement points are located at the same circumferential position with an outer tyre radius of (a) 0.26* m *(b) 0.32* m *(c) 0.4* m*.*

The response at a position away from the excitation point is shown in Fig. 6. This figure shows the vibration response also on the tyre centre-line but at a circumferential position *x/R* =1 where *x* is the distance around the circumference from the excitation

point and *R* is the tyre radius. Here the amplitude of the response is insignificant above 1 kHz and as before, an increase in the radius of the tyre moves the resonances to a lower frequency. This is useful as any excitation from the road surface or tread patterns above 700 Hz will not be radiated as significantly for the larger tyre.

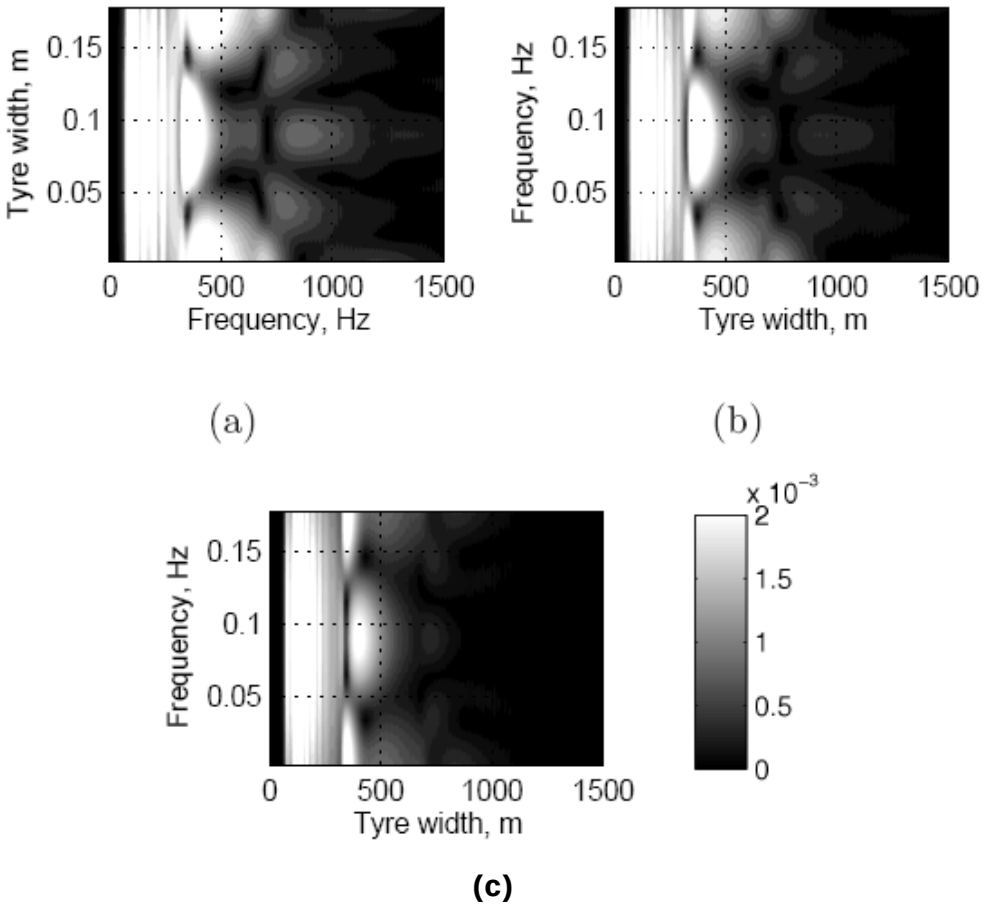

Fig. 6 As Fig. 5 but with the response is shown for a distance x/R =1 away from the excitation point

3.1.2 Modal response of the tyre with a change in the width of the tyre

The plots in Fig. 5 and 6 illustrate that as the excitation frequency increases different axial mode shapes can be seen across the tyre width, with an increasing number of nodes and anti-nodes. It is clear that a change in the width of the tyre will primarily change the wavelength of these modes. The complication arises due to the different damping factors in the sidewalls of the tyre and the damping due to bending in the tyre rubber. The radial velocity response along the centreline of the tyre is shown in Fig. 7 and the standard width tyre shows the largest amplitude response of all widths. This is because the increased damping from the sidewalls dominates for narrow tyres and the increased bending causes a larger proportion of the damping in the wider tyres. Therefore, for a reduction in exterior noise radiation we should alter the tyre width.

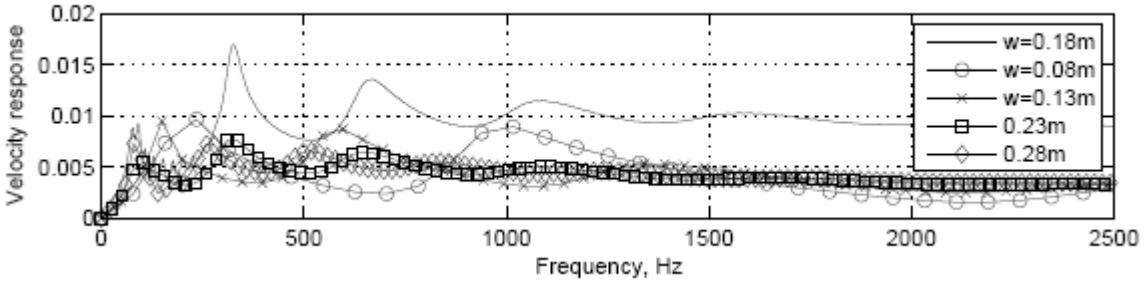

Fig. 7 Velocity response v_r / σ_{rr} *10* ^{9} m^3/Ns *of the tyre at the point of excitation for different width tyres. Excitation is applied on the tyre centre-line.*

The radial velocity response at the point of excitation (x = 0) is shown in Fig. 8 for a range of tyre widths and the effect of the sidewalls can be clearly seen. For the thinnest tyres, the response in the range 350 – 800 Hz is broadly zero, whereas for the standard tyre width resonances are extremely pronounced in this range. The amplitude of the resonances for the widest tyre are significantly less as the longer distances increase the amount of damping available to dissipate energy.

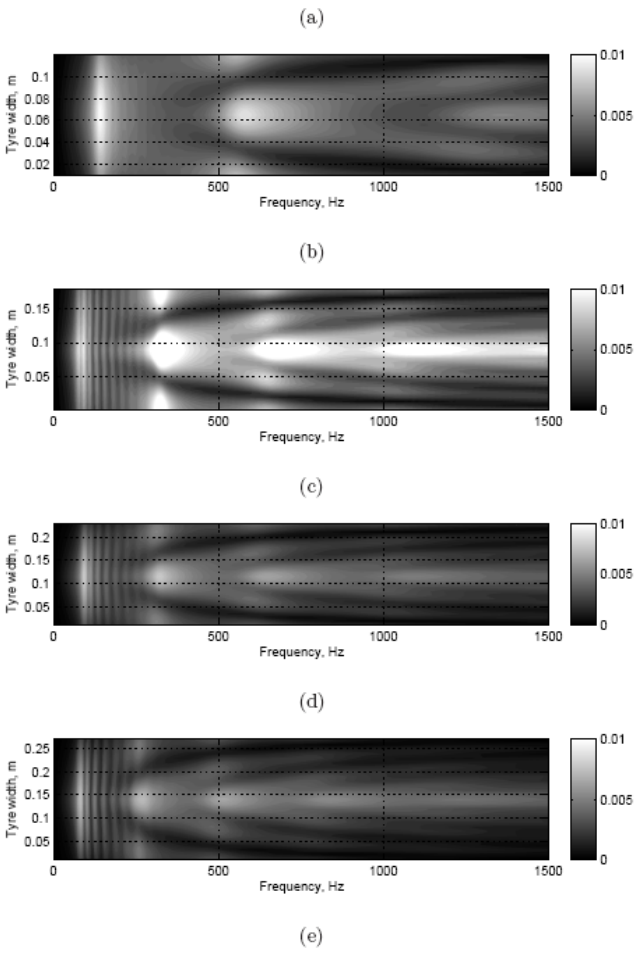

Fig. 8 Velocity response v_r / σ_{rr} 10 ^{9} m^3/Ns *of different width tyres. Excitation is applied on the tyre centre-line. Tyre widths respectively (a) 0.08* m *(b) 0.13* m *(c) 0.18* m *(d) 0.23* m *(e) 0.28* m.

This shows that reducing the tyre width slightly can have significant benefits provided the excitation from the tread pattern does not have too many impact frequencies in the range 550 – 600 Hz for common vehicle speeds in built up areas. It also illustrates the potential for developing a single layer across the width of the tyre which may be critically damped at the resonant frequency around 600 Hz.

The lowest mode is associated with the tyre moving up and down in the vertical plane at a frequency dependent on the stiffness of the sidewall springs and the tyre inflation pressure divided by the radius [13]. The resonance frequency of this mode can increase to 220 - 270 Hz, with a large amplitude response which would increase the noise in the passenger cabin (therefore an adequate damping solution would be required to mitigate this). However, in terms of exterior noise, this is not significant due to the A-weighting at low frequencies.

3.1.3 Effect of polyurethane in-fill

The mechanical response to a tyre can be changed significantly by a polyurethane in-fill. The vibration analysis of such a tyre fits naturally into the theoretical framework described in Section 2.1.1, which enables consideration of a tyre with a polyurethane material replacing the air cavity between the tyre belt and the wheel hub. Predictions for the modal velocity amplitude response of a polyurethane-filled tyre are shown in Figs. 9 and 10 and should be compared with results for a conventional tyre in Figs. 11 and 12. Figure 13 shows the response of a polyurethane tyre to point excitation.

For low angular (ie circumferential) orders and forcing frequencies less than 1 kHz, the dominant vibration mode involves surface waves of the polyurethane fill, with the tyre belt and tread moving on top of this thick layer with slight compression. However as the angular order becomes larger (and therefore the effective wavelength shorter), the dominant wave type changes into a flexural wave controlled by the stiffness of the belt and tread with the polyurethane effectively acting as a distributed spring bedding underneath the belt and tread. This resonance lasts for frequencies up to approximately 1.5 kHz. The amplitude of the resonant response at low angular orders and frequencies is significantly less than with an air cavity, an indication of the effectiveness of the damping in polyurethane. The velocity response of the polyurethane in-filled tyre for higher axial mode numbers is shown in Fig. 10. By comparison with Fig. 12, it may be seen that the polyurethane in-fill increases the cut-on frequency of a given axial mode. For illustration, the conventional tyre with an air cavity has a cut-on frequency of around 1.45 kHz for the axial mode of $m = 12$, and yet with the polyurethane in-fill the cut-on frequency of $m = 8$ is 1.4 kHz. As the axial mode number increases, the angular order at which the dominant wave type changes from the polyurethane surface wave to the tyre flexural wave decreases. However, the amplitude of the response for higher axial modes is slightly higher with the polyurethane in-fill. At very high angular orders, the compression of the tread rubber becomes more important in determining the response of the tyre, although the amplitude of response is then low enough not to warrant further comment.

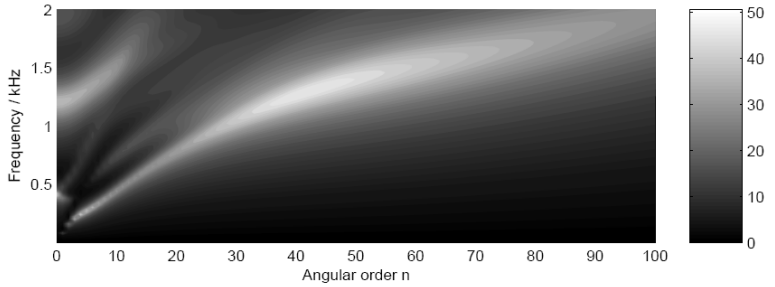

Fig. 9 Velocity response $v_r(r,\omega,n,m)/\sigma_{rr}$ *[m³/Ns] of the polyurethane- filled tyre belt and tread for the axial mode* $m=0$.

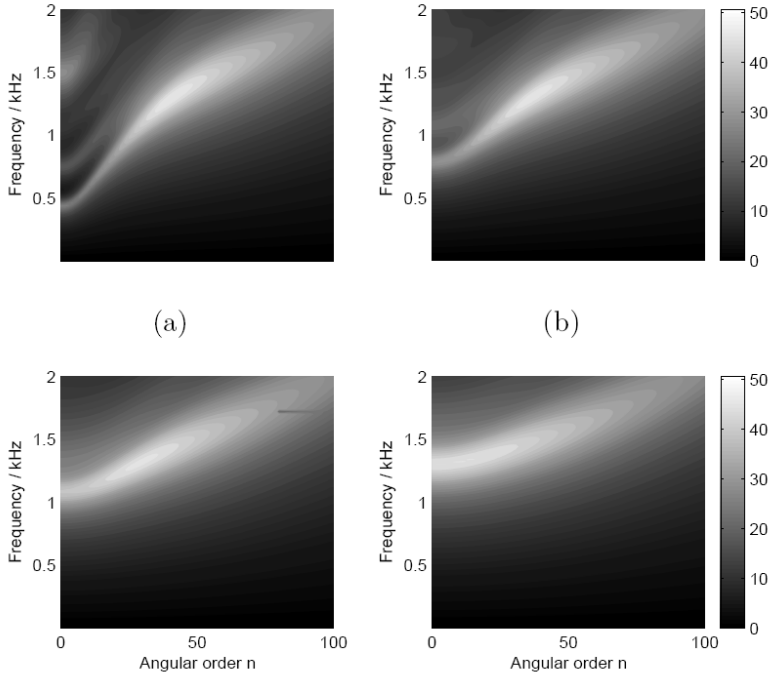

Fig. 10 As for Fig. 9 but for axial modes a) $m=2$*; b)* $m=4$*; c)* $m=6$*; and d)* $m=8$.

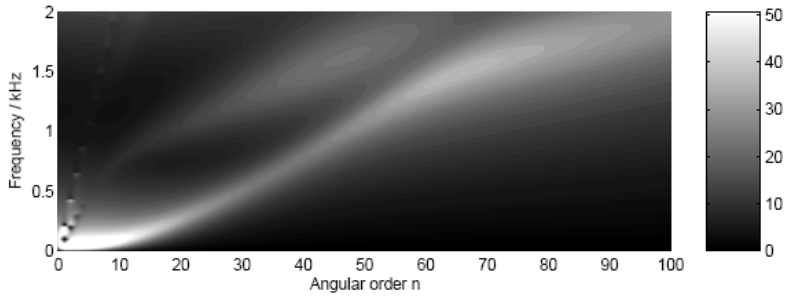

Fig.11 As Fig. 9 but for a conventional tyre with an air cavity

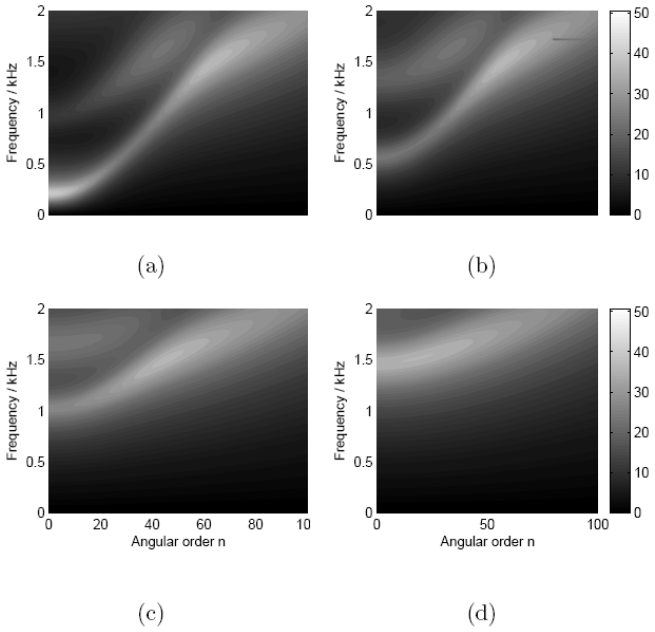

Fig.12 As Fig. 11 but for axial modes a) $m=3$*; b)* $m=6$*; c)* $m=9$*; and d)* $m=12$*.*

Figures 9-12 show the response of the different tyre structures in terms of the Fourier decomposition into angular and axial order and frequency. The response in the spatial domain of a polyurethane filled tyre is shown in Fig. 13. This is calculated by inverting the Fourier transforms. The results show the response for a position on the centre-line of the tyre in the span-wise direction and are plotted as a function of circumferential angle around the tyre. It can be seen that the vast majority of the vibration energy is close to the forcing point. Also noticeable is that the resonances are below 1.5 kHz and that those disturbances that do propagate away of the point of excitation tend to be for a forcing frequency below 1 kHz.

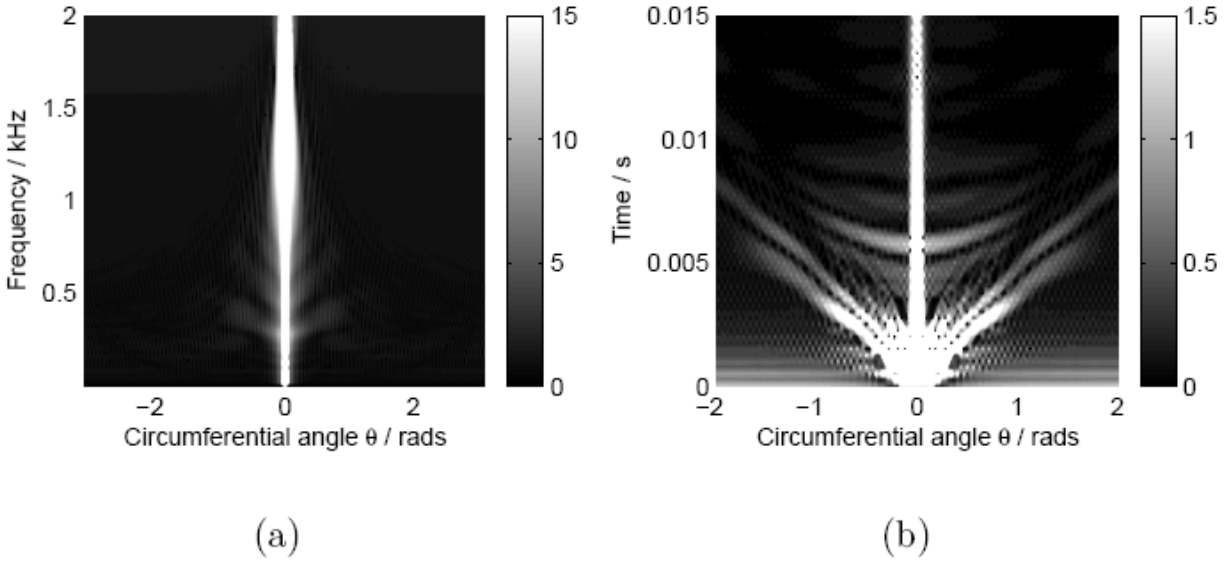

Fig. 13 Radial displacement response $u_r(r,t,\theta,0)/\sigma_{rr}$ *on the centre-line of the polyurethane filled tyre belt and tread*

Figure 14 shows mobility measurements made at the University of Cambridge comparing conventional air-cavity and polyurethane-filled tyres. It is clear that the amplitude of response of the polyurethane-filled tyre is lower at all frequencies except just around 630 Hz.

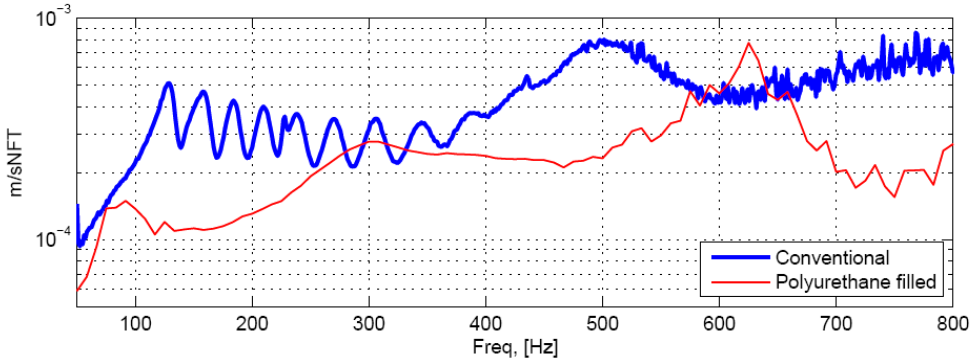

Fig. 14 Experimental measurements of the point mobility transfer function relating the velocity of the surface of the tyre along the centre-line to the force measurement v_r / σ_{rr} *[m/Ns] for a conventional air cavity and a polyurethane-filled tyre*

This reduction in point mobility and the rapid decay of radial displacements away from the point of excitation would lead to a significant reduction in noise. However, this is accompanied by an increase in weight of about 30 kg which is not practical. The weight increase could be reduced somewhat by reducing the thickness of the polyurethane layer and filling in between this layer and the wheel hub with spokes but instead we concentrated our novel tyre research on the twin-tyre concept which reduces both the tyre vibration due to the reduction in tyre width (see Section 3.1.2) and also a reduction in the horn amplification as will be discussed in Section 3.2.2.

3.1.4 Twin-Tyre Concept

The twin-tyre concept consists of two narrow tyres mounted on a single hub with the vibration of each tyre isolated. The vibration response of each tyre can be considered as an extreme example of the effect of a reduction in tyre width, as described in Section 3.1.2. Results are shown in Fig.15 comparing a conventional tyre of radius 0.32m and width 0.18m with a twin-tyre with each tyre of width 0.09m with all other parameters remaining constant (including sidewall stiffness). The overall reduction in vibration amplitude for the twin-tyre is noticeable and in the frequency range where the tyre-road excitation is most pronounced for (400-900Hz) the twin-tyre has only one resonance.

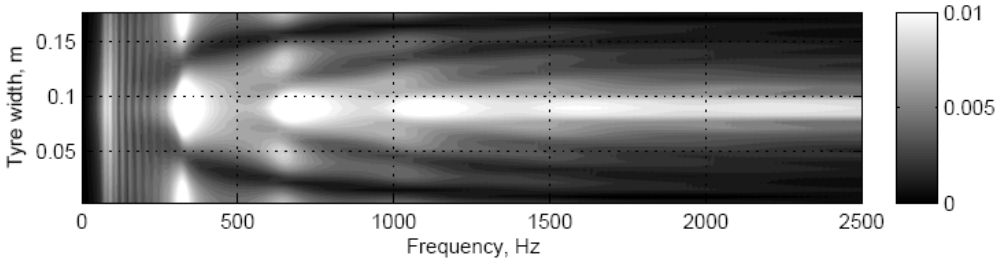

(a)

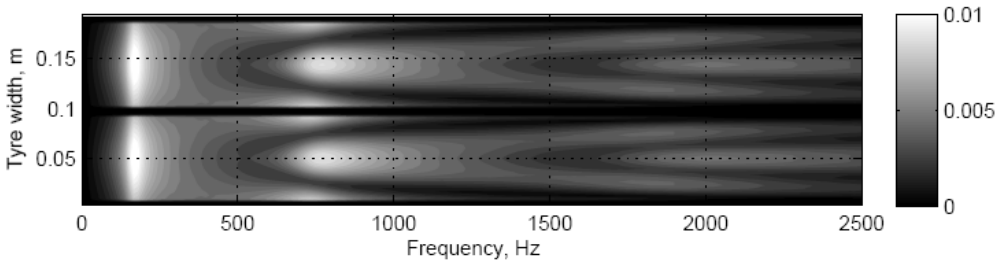

(b)

Fig. 15 Comparison of the velocity response at the forcing point of a) conventional and b) twin-tyre concept when excited at the centre of the tyres

3.2 SOUND FIELD

The far-field sound pressure has been calculated for a set of receiver positions illustrated in Fig. 16 for two speeds of 80 and 90 km/hr on a smooth and a hot rolled asphalt surface. The horn effect can be changed by small geometrical diiferences, for example by changes in the shoulder radius, and so we have presented results separately by firstly neglecting the horn amplification term in equation (4) and then showing separately results for the horn amplification.

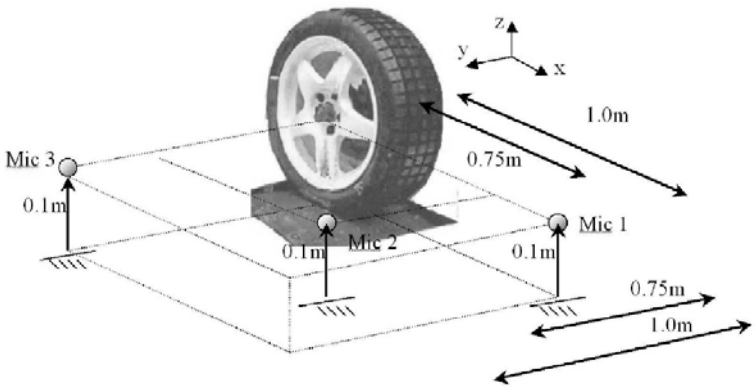

Fig. 16 The microphone positions

3.2.1 Effect of tyre radius

Results showing the effect of change in tyre radius are shown in Figs. 17 and 18.

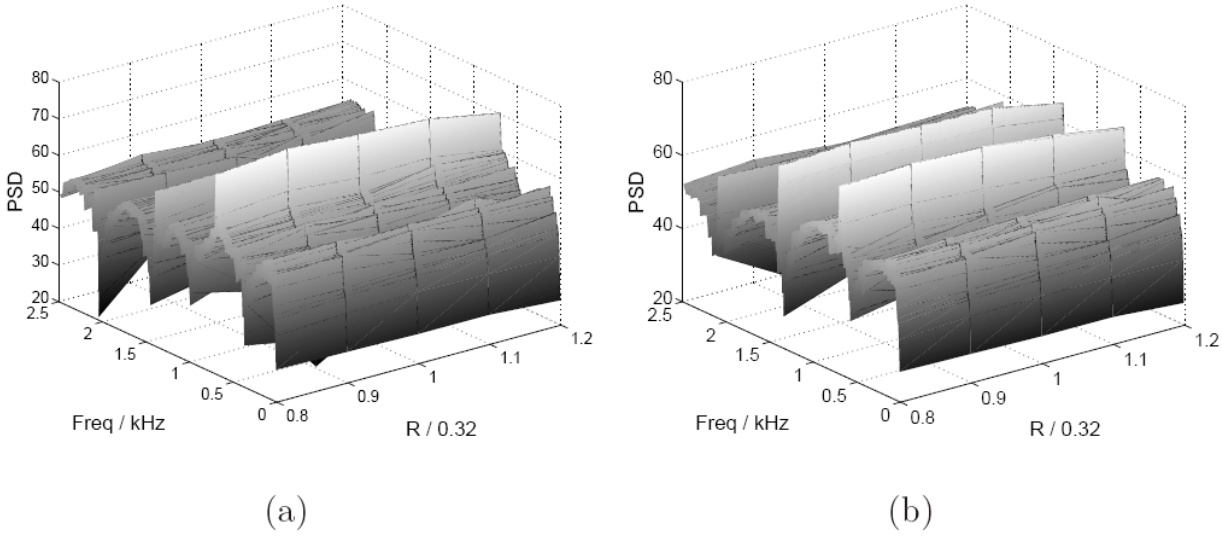

Fig. 17 Showing the effect of tyre radius on the power spectral density of the sound pressure [dB] calculated without the horn amplification on a smooth road surface at 90 km/hr, for a) Microphone Position 1; b) Microphone Position 2

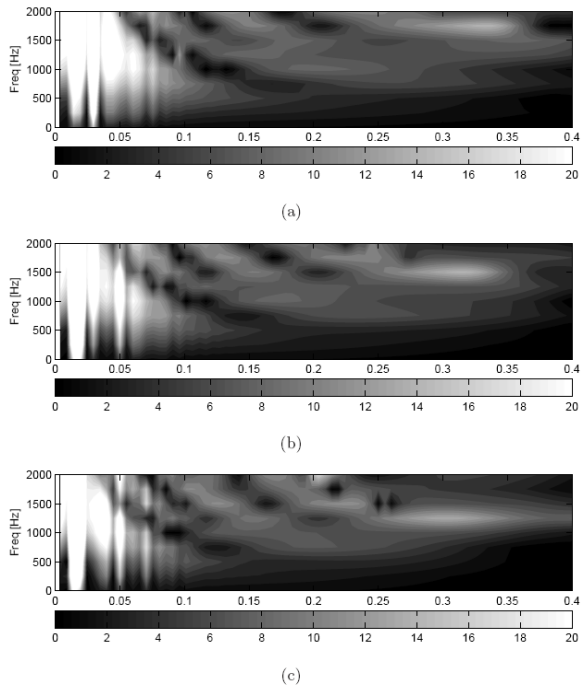

Fig. 18 Showing the effect of tyre radius on the horn amplification G_{horn} as a function of frequency and circumferential position x/R for Microphone Position 1.

Tyre radius a) 0.263m, b) 0.32 m, c) 0.4m.

There is a predicted decrease of noise of 4 dB for a tyre rolling on a smooth road surface between the smallest and largest radii tyres, before the horn effect is included. For the noise on a rough road surface, only a 1 dB decrease was found for moving from a standard tyre to the most extreme. The amplitude of the horn amplification is also altered by approximately 2-3 dB across the commercial size range. Increasing the radius lowers the frequency of maximum amplification. The reduction in the sound field from altering the tyre surface acceleration is cancelled somewhat when the horn effect is included.

3.2.2 Effect of tyre width

Results showing the effect of change in tyre radius are shown in Figs. 19 and 20.

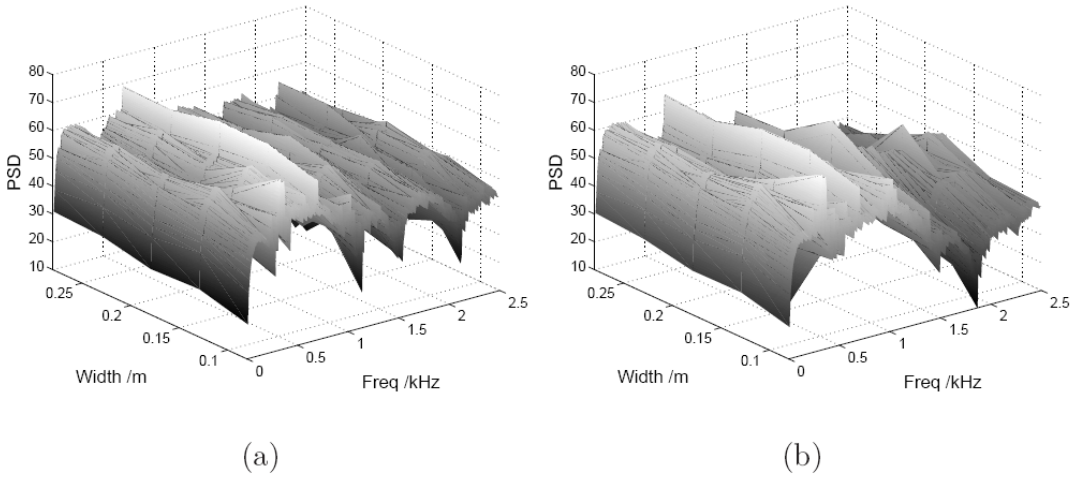

Fig. 19 Showing the effect of tyre width on the power spectral density of the sound pressure [dB] calculated without the horn amplification on a smooth road surface at 90 km/hr, for a) Microphone Position 1; b) Microphone Position 2

A tyre with a greater width has a longer axial wavelength and thus lower resonant frequencies. We saw in Section 3.1.2 that making a tyre narrower can move the modal response away from the typical range of excitation frequencies from the tread pattern. Although the load per unit area of a narrower tyre is increased, the amplitude of vibration is decreased significantly. Even when the horn effect is neglected, the far field sound pressure can be reduced by 4 dB by moving from the widest tyre to the narrowest as the resonant frequencies are located further away from the modal tyre response. Reducing the tyre width also has a significant decrease in the horn amplification. Over a commercial range of tyre widths, the decrease from the widest to the narrowest gives a further decrease of 3-5 dB, with significant shifts in the amplified frequencies below 1 kHz. This change shows the most potential for an engineering solution and hence further research was carried out on the twin-tyre concept.

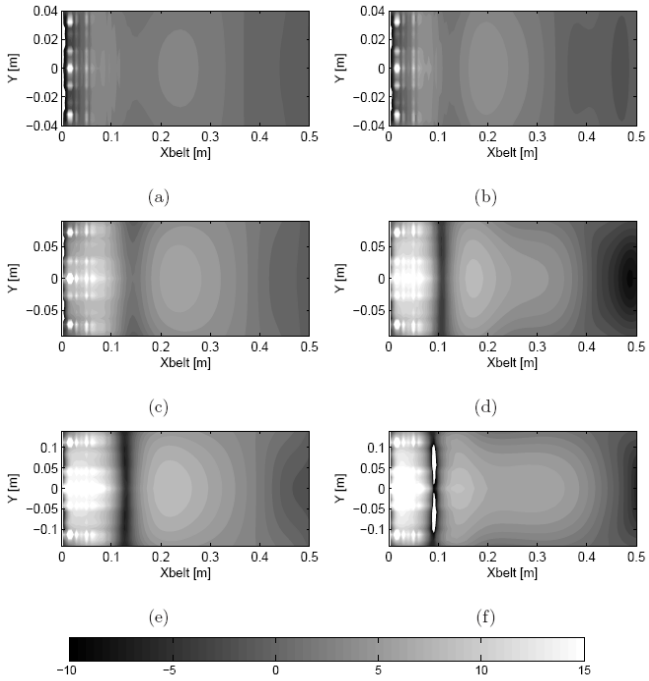

Fig. 20 Showing the effect of tyre width on the horn amplification G_{horn} as a function of frequency and circumferential position x/R for Microphone Position 1.

Results are shown for three tyre widths and two frequencies a) 0.08m, 0.75 kHz, b) 0.08m, 1 kHz, c) 0.18m, 0.75 kHz, d) 0.18m, 1 kHz, e) 0.28m, 0.75 kHz, f) 0.28m, 1 kHz.

3.2.3 Twin-tyre Concept

Results comparing the twin-tyre concept with a conventional tyre are shown in Figs. 21 and 22.

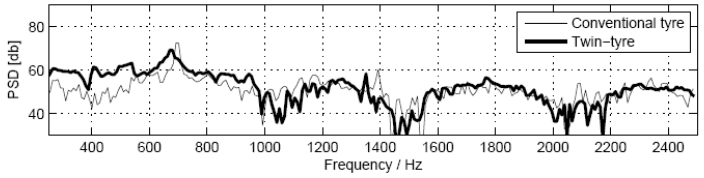

a) Microphone position 1

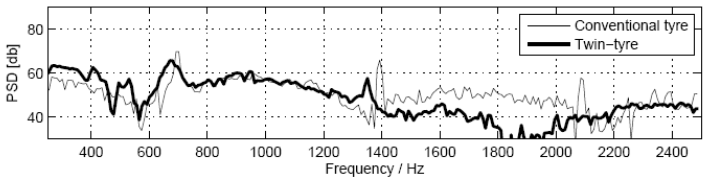

b) Microphone position 2

Fig. 21 Far-field sound pressure without the horn amplification of the twin-tyre concept and a conventional tyre on a smooth road surface at 90 km/hr for Microphone positions a) 1 and b) 2.

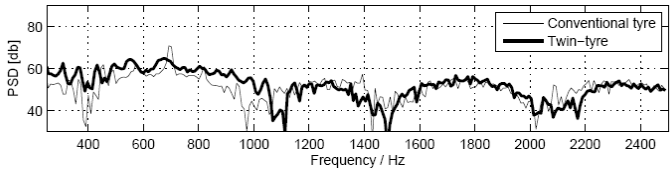

a) Microphone position 1

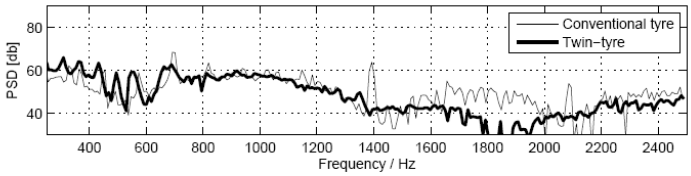

b) Microphone position 2

Fig. 21 As Fig. 20 but on a rough road surface

The corresponding horn amplification is shown in Fig. 22 and compared with that for a conventional tyre in Fig. 23.

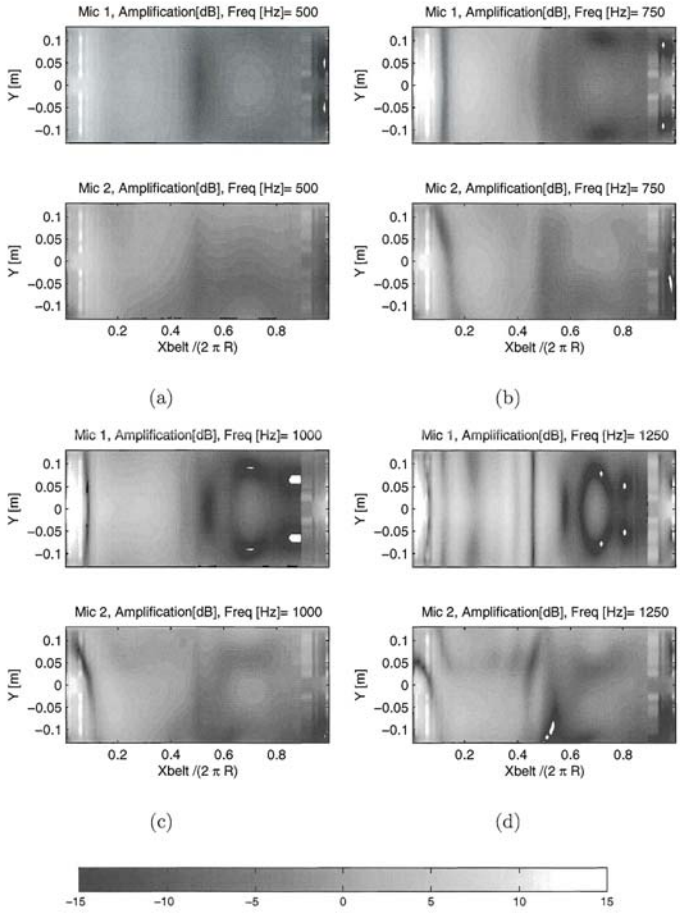

Fig. 22 The horn amplification G_{horn} as a function of frequency and circumferential position x_{belt}/R for the twin-tyre concept for two microphone positions and acoustic frequencies a) 500 Hz, b) 750 Hz, c) 1000 Hz and d) 1250 Hz.

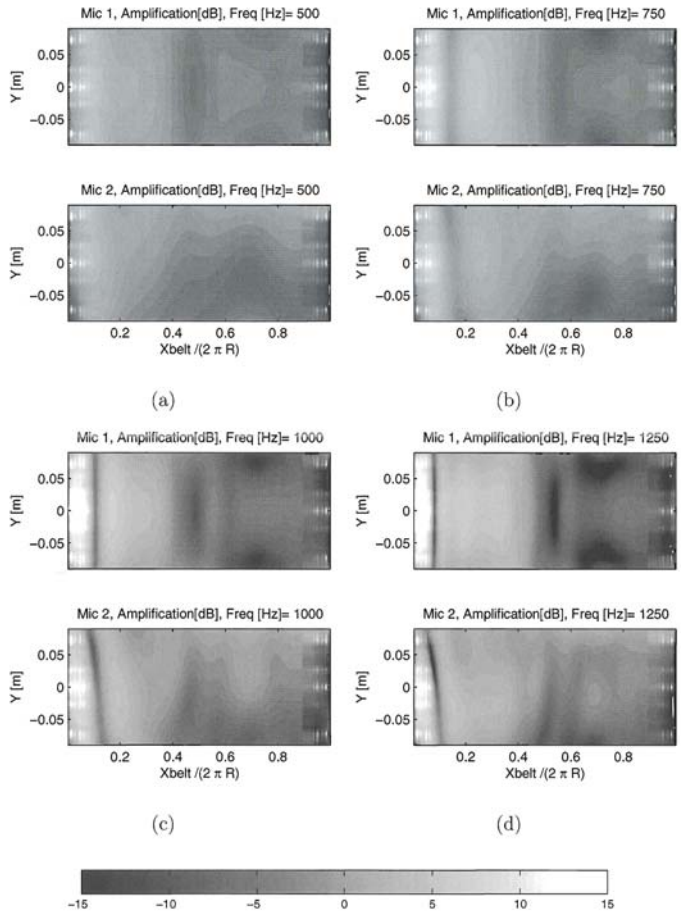

Fig. 23 As Fig. 22 but for a conventional tyre

A sound reduction of about 3.5 dBA is shown to be possible due to the modified modal response and the increase in damping between the two tyres. As the width of the tyre is reduced, the resonant frequencies decrease. With a single tyre this would not be practical because the load carrying capacity would be significantly reduced. The twin-tyre concept allows the load carrying capacity to remain constant by using two individual tyres mounted on the same hub.

The twin-tyre concept also alters the characteristics of the horn amplification with the result that the amplitude of frequencies around 500 Hz are increased by 2-3 dB with a corresponding decrease at frequencies above about 1 kHz. This reduction is additive (in dB) to any reduction obtained through the change in vibration response. There is potentially a large amplification at all frequencies at the centre of the twin tyres which must be eliminated using sound absorbent material between the tyres whose effect has not been included in the boundary element calculations. This sound absorbing material would need to be sufficiently durable and reliable for use in a commercial product.

An assessment of the effects of shoulder curvature on the horn amplification was also carried out. A reduction of approximately 1-2 dB results from a change from a tyre with square shoulders to one with a radius of curvature of 0.06m. An increase of shoulder radius to 0.09 m yields a reduction of 2-3 dB.

4 CONCLUSIONS

An investigation has been carried out into the potential noise reduction which can be obtained by varying the geometry of a passenger car tyre. It is assumed that for any change the overall load that the tyre will carry will remain constant.

Reducing the tyre radius reduces the mechanical vibration of the tyre but this is somewhat offset by an increase in the horn amplification. Reducing the tyre width has benefits for both a reduction in the mechanical vibration and the horn amplification. The twin-tyre concept provides a way of reducing the effective tyre width while maintaining the same overall load. An additional benefit is that such a concept leads naturally to tyre 'shoulders' of smaller radius of curvature, thereby reducing the horn effect still further.

5 REFERENCES

[1] Future noise policy, COM(96)540. European Commission, Green Paper, 1996.

[2] Tyre/road interaction noise: A 3d viscoeleastic multilayer model of a tyre belt, submitted for publication *J of Sound and Vibration*, D. O' Boy and A Dowling

[3] Tyre-road Noise. D. O' Boy, PhD thesis, University of Cambridge, 2005.

[4] Tyre-road interaction noise, R.A. Graf, PhD thesis, University of Cambridge, 2002.

[5] R.A. Graf, C.-Y. Kuo, A.P. Dowling, and W.R. Graham. Tyre/road interaction noise. *Proceedings of Internoise 2001*, 1, 2001.

[6] Understanding Road Generated Noise from Tyres (URGENT), A Dowling, W Graham and R Graf, IST-054 EPSRC GR/M09056/01 and GR/M11431/01, Tech Rep., Department of Engineering, University of Cambridge, 2002

[7] A mathematical model of tyre noise generation, W Kropp, Heavy Vehicle Systems, *International Journal of Vehicle Design*, **6**, 310-329, 1999

[8] Tyre/road noise generation – modelling and understanding, W Kropp, K Larsson, F Wullens and P Andersson, *Proc of the Institute of Acoustics*, 2004

[9] On the horn effect of a tyre/road interface - Part I: Experiment and computation R A Graf, C Y Kuo, A P Dowling and W R Graham, *Journal of Sound and Vibration*, **256**, 417-431. 2002.

[10] Boundary Element Techniques in Engineering, C Brebbia and S Walker, Newnes-Butterworths, 1980.

[11] The Boundary Element Method for Engineers, C Brebbia, Pentech Press, 1980.

[12] Sound and Sources of Sound, A P Dowling and J E Ffowcs Williams, Ellis Horwood, 1989.

[13] The vibration of rolling tyres in ground contact, S Huang, *International Journal of Vehicle Design*, **13**, 78-95, 1992.